

Numerical Simulation of Influence of the Thermal and Mechanical Fluctuations in the Coupling Elements of Microresonators

Vladislav I. Pavlov, Igor Yu. Blinov, Nickolay P. Khatyrev
Russian Metrological Institute of Technical Physics and Radio Engineering
Mendeleevo, Russia
pvi044@gmail.com

Nikita M. Kondratiev, Igor A. Bilenko
Russian Quantum Center
Skolkovo, Russia
noxobar@mail.ru

Abstract – Ultra-stable lasers of high spectral purity are the technological basis for optical atomic clocks, quantum measurements, stable microwave signal sources and high-resolution optical spectroscopy. For these purposes, lasers with a linewidth of the order of hertz are used. Such lasers are usually stabilized with Fabry-Perot resonators made of ultra-low expansion materials, which are very fragile and bulky. Therefore, there is a clear demand for reliable miniature lasers with narrow linewidths. Optical resonators with a “whispering gallery” mode (WGM) make it possible to create narrow-band microlasers on their basis using self-injection locking method. But they have not yet reached the stability determined by their fundamental noise. Here we calculate the noise characteristics of lasers self-injection locked to WGM microresonators and estimate the linewidth limitations due to thermorefractive, thermoelastic, photoelastic and Brownian noise. We also calculated the total noise in an integrated waveguide and obtained an estimate of the linewidth of 0.5 kHz at an averaging time of 1 s.

Keywords – microresonator, laser stabilization, self-injection locking, thermorefraction

I. INTRODUCTION

Stable narrow-linewidth lasers are of great importance for many applications in science and technology, such as length metrology, high-resolution spectroscopy and atomic clocks [1]. One of the effective methods of diode laser stabilization and linewidth reduction is the self-injection locking to a high-Q “whispering gallery” mode (WGM) microresonators. The linewidth reduction of more than a thousand times was shown experimentally with this technique [2]. However, there are questions about the limit of such stabilization. It was shown [3] that the frequency fluctuations $\delta\nu$ of the laser diode depend on the fluctuations of the optical path of laser beam δD in the coupling element:

$$\delta\nu = \frac{\omega_m^2}{2Q_m c} \delta D, \quad (1)$$

This work was supported by the Russian Science Foundation (project 20-12-00344).

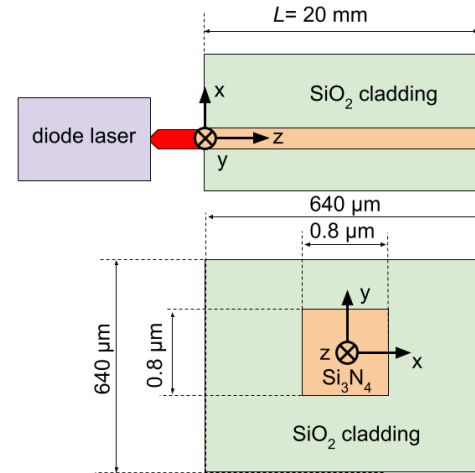


Fig. 1. Integrated waveguide model used in finite element method simulation.

where $D = \int_L n_{\text{eff}}(\vec{r}) dz$ is optical path between diode laser and microresonator, $n_{\text{eff}} = 1.72$ – effective refraction index of the optical path, ω_m is the eigenfrequency of the microresonator mode, Q_m is Q-factor of the microresonator mode. In our case, the coupling element with the microresonator is the integrated waveguide, shown in the Fig. 1. Thus, we related the fluctuations of the laser frequency fluctuations and the fluctuations of the refractive index of the waveguide:

$$\delta\nu = \int_V \frac{\omega_m^2}{2Q_m c} \frac{\delta n_{\text{eff}}(\vec{r})}{S} dV, \quad (2)$$

where $S = 0.8 \mu\text{m} \times 0.8 \mu\text{m}$ is the cross-sectional area of the integrated waveguide.

II. FLUCTUATION-DISSIPATION THEOREM METHOD

Waveguide noise calculation is based on the fluctuation-dissipation theorem (FDT). FDT is a theorem of statistical physics that connects system fluctuations (spectral density) with dissipative properties [4]. FDT is derived from the assumption that the response of the system to a small external action is the same nature as the response to fluctuations.

We consider a linear system, described by the generalized coordinate x and observable y . Let the system be acted upon by a weak periodic generalized force $f = F_0 \cos(\omega t) q_f(r)$, where $q_f(\vec{r})$ is the form-factor determined by the relation between the coordinate and the observable:

$$y = \int_V x(\vec{r}) q_f(\vec{r}) dV \quad (3)$$

We can calculate the response x of the system and dissipative power $W_{\text{diss}}(f)$. Thus, the spectral density of fluctuations of the observable y is determined by the expression:

$$S_y(\omega) = \frac{4k_B T}{\omega^2 F_0^2} W_{\text{diss}} \quad (4)$$

In our case, the observable is the frequency fluctuation $\delta\nu$ of the laser diode self-injection locked to a integrated microresonator, F_0 – normalization constant, ω – Fourier frequency.

A. Thermorefractive Noise

Temperature fluctuations lead to fluctuations in the refractive index of the waveguide through the thermo-optic coefficient $\beta_{\text{eff}} = dn_{\text{eff}}/dT$. We chose the temperature deviation δT as the generalized coordinate and the entropy s as the generalized force. Thus, we can write for the observable laser frequency fluctuation $\delta\nu$:

$$\delta\nu = \int_V \frac{\omega_m^2}{2Q_m c} \frac{\beta_{\text{eff}} \delta T(\vec{r})}{S} dV \quad (5)$$

It can be seen that the structure of the formula (5) corresponds to the structure of the formula (3). Therefore, the form factor for thermorefractive noise at the observable $\delta\nu$ is expressed:

$$q_f(\vec{r}) = \frac{\omega_m^2 \beta}{2SQ_m c} \quad (6)$$

Temperature obeys the heat transfer equation:

$$\delta Q - \text{div } j \delta T = T \delta s. \quad (7)$$

We take into account that δT and \dot{s} are small, in the first order of approximation and $\delta T = \text{Re}[\tilde{T} e^{-i\omega t}]$. As a result, we obtain a system of equations for numerical simulation using the finite element method.

$$\begin{cases} i\omega \rho C_v \tilde{T} + k \Delta \tilde{T} = i\omega T_0 F_0 \frac{\omega_m^2 \beta}{2SQ_m c} \\ \tilde{T}|_{\infty} = 0, \end{cases} \quad (8)$$

We calculate the dissipative thermal power in the integrated waveguide using the expression:

$$W_{\text{diss}} = \int \frac{\kappa}{T} (\text{grad } \delta T)^2 dV \quad (9)$$

As result, the spectral density of laser frequency fluctuations caused by thermorefractive noise has the form:

$$S_{TR}(\omega) = \frac{4k_B T}{\omega^2 F_0^2} \int \frac{\kappa}{T} (\text{grad } \delta T)^2 dV, \quad (10)$$

B. Brownian Noise

Brownian noise is caused by fluctuations of the mechanical stress in a material. For Brownian noise, the generalized coordinate is the displacement field x , and the generalized force is the force \vec{F} . Thus, we can write for the observable laser frequency fluctuation $\delta\nu$:

$$\delta\nu = \int \frac{n_{\text{eff}} \vec{n}_{\perp} \vec{u}}{S} \frac{\omega_m^2}{2Q_m c} \delta(S_w(\vec{r})) dV, \quad (11)$$

$S_w(\vec{r})$ is a function that defines a surface. It is equal to zero when the point \vec{r} lies on the surface, \vec{n}_{\perp} is unit normal vector to the surface. Form factor for Brownian noise at the observable $\delta\nu$ is expressed:

$$q_f(\vec{r}) = \frac{n_{\text{eff}}}{S} \frac{\omega_m^2}{2Q_m c} \vec{n}_{\perp}, \quad (12)$$

We solved the equation of elastic vibrations in the frequency domain in the form $\vec{u}(t) = \text{Re}[\vec{u} e^{-i\omega t}]$:

$$\begin{cases} -\rho \omega^2 \vec{u} - \nabla(\hat{\sigma}) = 0 \\ \hat{\sigma} \vec{n}_{\perp}|_S = F_0 \frac{n}{S} \frac{\omega_m^2}{2Q_m c} \vec{n}_{\perp} \end{cases} \quad (13)$$

where ρ is the material density, $\omega = 2\pi f$ is the Fourier frequency, $\hat{\sigma}$ is the tensor of mechanical stresses, \vec{u} is the deformation field, F_0 is the normalization constant. The dissipative mechanical power in the system is determined by the formula:

$$W_{\text{diss}} = \omega \phi_0 \int \sum_{ij} \epsilon_{ik} \sigma_{ik} dV \quad (14)$$

where ϵ_{ik} and σ_{ik} are the components of the tensors of deformations and mechanical stresses, respectively, ϕ_0 is the tangent of the angle of mechanical losses. As a result, the spectral density of laser frequency fluctuations caused by Brownian noise has the form:

$$S_{BR}(\omega) = \frac{4k_B T}{\omega F_0^2} \phi_0 \int \sum_{ij} \epsilon_{ik} \sigma_{ik} dV, \quad (15)$$

C. Thermoelastic Noise

Thermoelastic noise is related to the coefficient of thermal expansion $\alpha = dL/dT$. Note that in FTD it is not required that the considered losses correspond to the generalized coordinate. In case of thermoelastic noise, it is convenient to take the displacement field as a generalized coordinate and the mechanical force acting on the waveguide as the generalized force. Moreover, Form-factor shape is the same as the Brownian noise:

$$q_f(\vec{r}) = \frac{n_{\text{eff}}}{S} \frac{\omega_m^2}{2Q_m c} \vec{n}_{\perp} \quad (16)$$

We solved the thermoelasticity and heat transfer equation together:

$$\begin{cases} -\rho \omega^2 \vec{u} - \nabla(\hat{\sigma}) = 0 \\ \hat{\sigma} \vec{n}_{\perp}|_S = F_0 \frac{n}{S} \frac{\omega_m^2}{2Q_m c} \vec{n}_{\perp} \\ i\omega \rho C_v \tilde{T} + k \Delta \tilde{T} = i\omega T_0 \alpha_{ij} \sigma_{ij} \\ \tilde{T}|_{\infty} = 0 \end{cases} \quad (17)$$

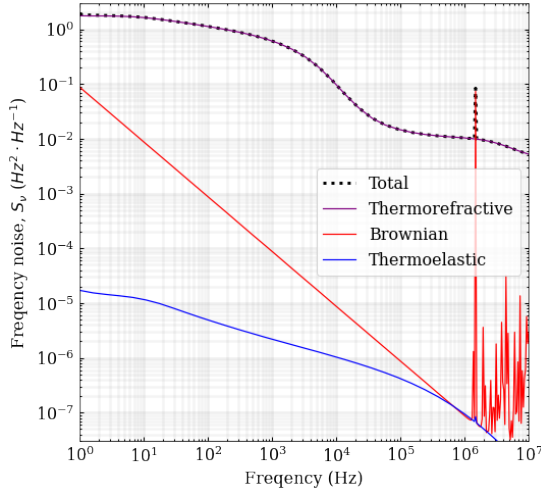


Fig. 2. Numerical simulation of the total noise (black dotted curve) in a waveguide including thermorefractive (purple curve), thermoelastic (blue curve), and Brownian noise (red curve). Note that the photoelastic noise turned out to be much less than the other contributions due to the small photoelasticity coefficient of Si_3N_4 .

TABLE I
PHYSICAL PROPERTIES OF WAVEGUIDE MATERIAL USED FOR FEM SIMULATIONS

| Physical properties | Si_3N_4 | SiO_2 |
|---|-------------------------|---------------------|
| Density ρ (kg/m^3) | $3.29 \cdot 10^3$ | $2.20 \cdot 10^3$ |
| Refractive index n | 1.996 | 1.44 |
| Thermo-optic coefficient β ($1/\text{K}$) | $2.4 \cdot 10^{-5}$ | $9.4 \cdot 10^{-6}$ |
| Thermal conductivity k ($\text{W/(m} \cdot \text{K)}$) | 30 | 1.4 |
| Specific heat capacity C ($\text{J/(kg} \cdot \text{K)}$) | 800 | 730 |
| Young's modulus E (Pa) | $250 \cdot 10^9$ | $70 \cdot 10^9$ |
| Poisson's ratio μ | 0.23 | 0.17 |
| Thermal expansion coefficient α ($1/\text{K}$) | $2.3 \cdot 10^{-6}$ | $0.5 \cdot 10^{-6}$ |
| Mechanical loss factor ϕ_0 | $8 \cdot 10^{-5}$ | $4 \cdot 10^{-5}$ |

After that, We calculate losses in the same way as in thermorefractive noise (9). Note that while the entropy change is applied to the volume, all forces got were applied to the guide surfaces.

III. RESULTS

Fundamental noises in integrated Si_3N_4 waveguides were simulated using the finite element method. For this purpose, we used physical properties of waveguide material from the TABLE I. Fig. 2 shows that the thermorefractive noise dominates in integrated waveguides at frequencies of $1 - 10^7$ Hz. This result is similar for the case with integrated Si_3N_4 microresonators noise [5].

Then, we compared the noise in the integrated waveguide with the noise in integrated microresonators with $\text{FSR} = 1$ THz, 150 GHz and 5 GHz calculated using finite element method. It can be seen in Fig. 3 that the noise of the microresonator decreases with decreasing the FSR (that is, with increasing the radius of the microresonator). However, Fig. 3 shows that the total noise in the integrated waveguide is negligible compared to the noise of integrated microresonators.

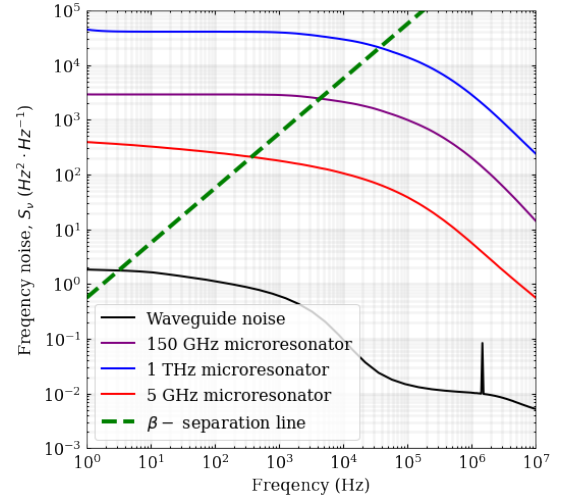


Fig. 3. Comparison of the frequency noise of integrated microresonators (black curve) with different FSRs (1 THz – blue curve, 150 GHz – purple curve, 5 GHz – red curve) and integrated waveguide of length $L = 20$ mm. Green dashed line is β -separation line $S_\beta(f) = 8 \ln(2)f/\pi^2$ [9].

The frequency noise level of integrated waveguide is about $10^{-2} \text{ Hz}^2 \cdot \text{Hz}^{-1}$ at MHz frequencies being less than [6] results over 100 times.

One of the most common characteristic of lasers is linewidth. There are several different methods to estimate the linewidth from the spectral density of the frequency noise. The maximum laser linewidth due to noise in the integrated waveguide from Fig. 1 was estimated as a frequency excursion (see (3.74) from [7], Chapter 3):

$$\Delta\nu_{\text{rms}} = \sqrt{\int_{\frac{1}{\tau}}^{f_c} S_\nu(f) df}, \quad (18)$$

where τ is an averaging time (measurement time), f_c is high-frequency cutoff frequency. Using $\tau = 1$ s, $f_c = 5$ MHz we get $\Delta\nu_{\text{rms}} \sim 0.5$ kHz.

The short-term linewidth, used in [6] can be considered as an estimate of the minimum possible linewidth (see (3.70) from [7], Chapter 3):

$$\Delta\nu = \pi S_\nu(f_c). \quad (19)$$

This estimation for $f_c = 5$ MHz gives us $\Delta\nu \sim 10^{-1}$ Hz.

Another effective linewidth $\Delta\nu_{\text{eff}}$ calculated method provides an integral equation to be solved [8]:

$$\int_{\Delta\nu_{\text{eff}}}^{\infty} \frac{S_\nu}{f^2} df = \frac{1}{\pi}. \quad (20)$$

Such estimation gives $\Delta\nu_{\text{eff}} \sim 4$ Hz that is more than results [6]. We also estimated the linewidth $\Delta\nu_\beta \sim 3$ Hz using the β -separation line method [9], which is in good agreement with (20).

It can be seen that different methods for estimating the linewidth can give different results and therefore it is always necessary to specify the method by which the linewidth was calculated especially for commercial products.

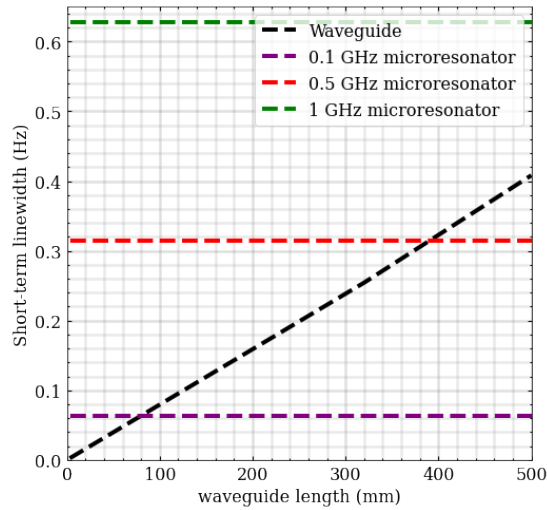


Fig. 4. Dependence on the length of the short-term linewidth (19) corresponding to the frequency noise level at frequencies of 5 MHz of the integrated waveguide (black dashed line). Integrated microresonators with FSR = 0.2 GHz (purple), 0.5 GHz (red), 1 GHz (green) short-term linewidth (19) (horizontal dashed lines) corresponding to the frequency noise level at frequencies of 5 MHz.

Finally, we study the noise dependence on the waveguide length. Fig. 4 shows that waveguide contribution to the short-term linewidth defined by equation (19) is linearly proportional to the waveguide length. We can see that the bus guide noise becomes significant for microresonators at certain lengths. Therefore, it is necessary to take it into account when using waveguides with a length of more than 100 mm.

IV. DISCUSSION

Despite the fact that our results show that the noise in the waveguide is negligible in the 1 THz - 5 GHz FSRs range, there are regions where waveguide noise become significant. In particular, meter spiral waveguides were demonstrated in the work [10]. Such waveguides should have a higher noise level and it will become necessary to take noises in waveguide into account.

Also, integral waveguides are sometimes used as a coupling element with disk WGM microresonators [11]. Disk microresonators have a lower noise level compared to integrated microresonators due to the possibility of using materials with a lower thermo-optical coefficient. Therefore, the mathematical models presented in this work should also be used for simulating systems with disk microresonators.

In fact, it is more correct to compare the frequency noise values at different frequencies (spectral density curves), as the measured linewidth usually depends on the measuring device (integration time, cutoff frequency etc.). For example, a disk microresonator in [12] had a frequency noise of the order of $1 \text{ Hz}^2 \cdot \text{Hz}^{-1}$ at frequencies of 10^3 Hz , which is lower than measured in the integrated microresonator [6] ($10^4 \text{ Hz}^2 \cdot \text{Hz}^{-1}$ at frequencies of 10^3 Hz) despite the fact that the linewidth measured in the disk microresonator was equal to 25 Hz [12]

versus 1.2 Hz in the integrated microresonator [6]. That is, the linewidth depends on the device, the measurement technique, the averaging time and other conditions.

V. CONCLUSIONS

In this work the thermorefractive, thermoelastic and Brownian noises in the coupling elements for high-quality-factor ($Q_m = 10^7$) integrated silicon-nitride microresonator were calculated using the fluctuation-dissipation theorem and the finite element method. The simulations were performed for a ($S = 0.8 \text{ } \mu\text{m} \times 0.8 \text{ } \mu\text{m}$) silicon-nitride waveguide of 20 mm length at wavelength $1.5 \text{ } \mu\text{m}$. It was found that for the integrated waveguide the linewidth limit imposed by thermal noise of the coupler optical path is at the level of 0.5 kHz at an averaging time of $\tau = 1 \text{ s}$. Based on the simulation it was concluded that the experimental results obtained, for example, in the study [13] 1 kHz is limited by other fluctuation processes.

REFERENCES

- [1] Z. L. Newman, V. Maurice, T. Drake, et. al. "Architecture for the photonic integration of an optical atomic clock," *Optica* vol. 6, pp. 680-685, 2019.
- [2] N.G. Pavlov, S. Koptyaev, G.V. Lihachev et. al. "Narrow-linewidth lasing and soliton Kerr microcombs with ordinary laser diodes." *Nature Photonics* vol. 12, nr. 11, pp. 694-698, October 2018.
- [3] N. M. Kondratiev, V. E. Lobanov, A. V. Cherenkov, et. al., "Self-injection locking of a laser diode to high-Q WGM microresonator." vol. 25, nr. 23, p. 28167-28178, 2017.
- [4] N.M. Kondratiev and M.L.Gorodetsky, "Thermorefractive noise in whispering gallery mode microresonators: analytical results and numerical simulation," *Physics Letters A*, vol. 382, nr. 33, p. 2265-2268, August 2018.
- [5] G. Huang, E. Lucas, J. Liu, et. al., "Thermo-refractive noise in silicon nitride microresonators," in *Conference on Lasers and Electro-Optics, OSA Technical Digest*, June 2019.
- [6] W. Jin, QF. Yang, L. Chang, et. al., "Hertz-linewidth semiconductor lasers using CMOS-ready ultra-high-Q microresonators." *Nat. Photonics* 15, 346-353, February 2021.
- [7] F. Riehle "Frequency Standards: Basics and Applications," Wiley-VCH, Weinheim, 2004
- [8] R. R. Galiev, N. G. Pavlov, N. M. Kondratiev, et. al., "Spectrum collapse, narrow linewidth, and Bogatov effect in diode lasers locked to high-Q optical microresonators," *Opt. Express* vol. 26, pp. 30509-30522, 2018.
- [9] G. D. Domenico, S. Schilt, and P. Thomann, "Simple approach to the relation between laser frequency noise and laser line shape," *Appl. Opt.* vol. 49, pp. 4801-4807, 2010.
- [10] J. Liu, G. Huang, R.N. Wang, et. al., "High-yield, wafer-scale fabrication of ultralow-loss, dispersion-engineered silicon nitride photonic circuits". *Nat Commun*, vol. 12, pp. 2236, April 2021.
- [11] V. R. Almeida, Roberto R. P., and M. Lipson, "Nanotaper for compact mode conversion," *Opt. Lett.* vol. 28, pp. 1302-1304, 2003.
- [12] J. Lim, A.A. Savchenkov, E. Dale, et. al., "Chasing the thermodynamical noise limit in whispering-gallery-mode resonators for ultrastable laser frequency stabilization," *Nat Commun* vol. 8, pp. 8, March 2017.
- [13] A.S. Raja, A.S. Voloshin, H. Guo, et. al., "Electrically pumped photonic integrated soliton microcomb." *Nat Commun* vol. 10, pp. 680, February 2019.